FLEXURAL PERFORMANCE OF HYBRID MULTI-GIRDER BRIDGE DECK WITH ALL-GFRP TRANSVERSE COMPOSITE ACTION SYSTEM

D. Chen[a], R. El-Hacha[a*]

[a] *University of Calgary, Department of Civil Engineering, 2500 University Drive N.W. Calgary Alberta T2N 1N4 Canada*
** relhacha@ucalgary.ca*

Keywords: hybrid bridge, post-tensioning, FRP, UHPC.

Abstract
This paper details the experimental testing of a 3m long hybrid bridge deck system built-up using FRPs and UHPC, with a transverse composite action system composed of horizontal and diagonal GFRP threaded rods. Results under both concentric and eccentric four-wheel loading configurations demonstrated good overall performance of the hybrid bridge deck system when subjected to service and ultimate loading conditions. Under ultimate loading, a progressive failure mechanism (pseudo-ductile behavior) was achieved, with a sustained load resistance above 70% of the maximum load after peak. The tensile strain induced in the horizontal GFRP rods resulted in less than 50% of the ultimate tensile strain in the rods, indicating that greater optimization of the design can be attained. Consistent load distribution was observed between adjacent parallel girders where the most eccentric loading configuration resulted in approximately 50% distributed load to the outer girder.

1. Introduction

Research and development into the use of high performance composite materials in the field of structural engineering has generated very exciting results in recent years. Applications for the use of Fiber Reinforced Polymers (FRPs) and Ultra-High Performance Concrete (UHPC) has expanded greatly from its research origins, which focused mainly on strengthening and rehabilitation purposes. In recent years, innovative designs for all FRP structures [7] as well as hybrid structures [10] have gained greater attention. This is mainly due to their appealing properties, which includes high strength-to-weight ratio, resistance to corrosion, and a high level of customization available to suit individual construction needs. For bridge applications, the development of an all-composite bridge deck system can be highly advantageous, particularly in locations with heavy traffic volumes, low overhead clearance or heavy usage of deicing salts. This paper will discuss the experimental test results obtained from a steel-free, all-composite hybrid multi-girder bridge deck system that includes a transverse composite action system composed solely from GFRP threaded rods. Discussion will focus on the following aspects: 1) the performance of the hybrid bridge deck system when subjected to concentric and eccentric wheel loadings under service loading conditions, 2) the exhibited failure mode of the hybrid bridge deck system at ultimate loading condition, 3) the behavior and efficiency of the transverse composite system, and 4) the degree of load distribution between parallel girders.

2. Bridge Design Concepts and Properties

The design and testing of the hybrid bridge deck system is the final stage in a multi-step project [2, 4-6, 9]. The cross-section, as shown in Figure 1, is composed of four GFRP hollow box beams integrated together with a cast-in-place UHPC top slab and reinforced with a Carbon FRP (CFRP) sheet along the outer face of each bottom flange. The longitudinal configuration of the bridge deck system, also shown in Figure 1, consists of a series of transverse unbonded post-tensioned (PT) rods, unbonded (non-prestressed) straps, and bonded diaphragm cross-braces, using solely 5/8' threaded GFRP rods, provided at regular spacing along the length of the bridge system. To promote greater bond between the GFRP beams and the UHPC slab, a specially designed epoxy bonded coarse silica sand aggregate layer [5] was used along with bonded vertical GFRP rods. To reinforce the areas where vertical and transverse rods were located, UHPC stiffener blocks were cast into the interior of the GFRP girder. These transverse structural components were designed using adapted guidelines from CSA S6-06 [3] and experimental test results relating to the performance of PT GFRP rods [6].

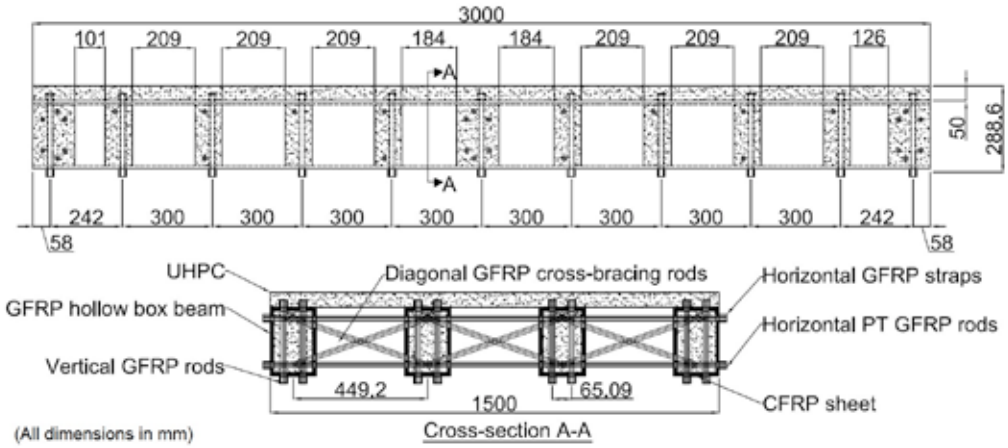

Figure 1. Elevation view of hybrid bridge deck system with cross-sectional view at mid-span

A summary of the relevant material properties is provided in Table 1.

Material	Tension Properties		Compression Properties	
	Strength [MPa]	Modulus of Elasticity [MPa]	Strength [MPa]	Modulus of Elasticity [MPa]
GFRP beam [4, 9]	207	17200	–	–
CFRP [4, 9]	986	95800	–	–
GFRP threaded rod [6]	94	13790	–	–
UHPC [4, 9]	–	–	150-180	50000-60000

Table 1. A selection of properties for materials used in hybrid bridge deck system design

3. Experimental Program

Experimental testing was conducted using service and ultimate loading conditions. Service loading was applied through various four-wheel loading configurations to ascertain the interactions between the different structural components in the system as well as to identify the distribution of load between adjacent girders. The applied loading regime for all service condition configurations were determined based upon guidelines found in ACI 437.1R-07 [1]. A similar quasi-static loading regime was applied during the initial stages of the ultimate load condition test. The service and ultimate loading regimes are presented in Figure 2.

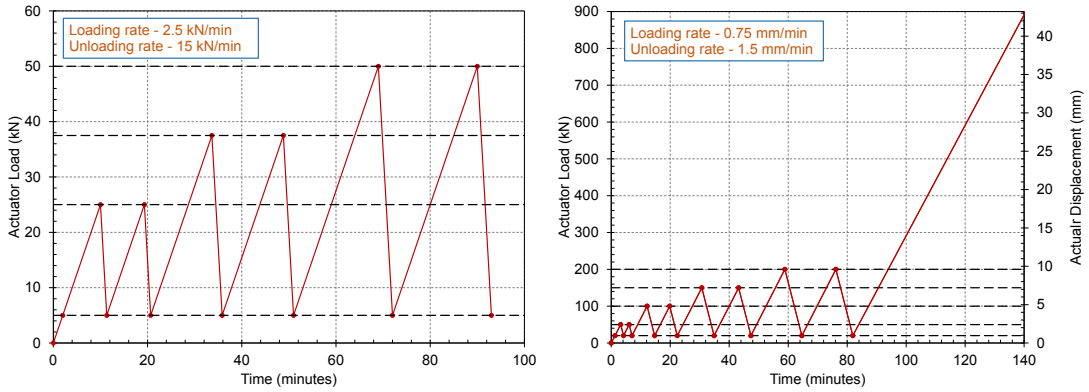

Figure 2. Loading regimes for service loading tests (left) and for ultimate loading test (right)

The spacing between the wheel loadings in the longitudinal direction for all loading configurations was 600 mm, centered about the load actuator. The four-wheel loading configuration was achieved through with a 1 MN actuator and an assembled double spreader beam system with a spherical seat between the top spreader beam and the actuator. The wheel load positions for each load configuration are provided in Table 2.

Concentric Configurations	**Eccentric Configurations**	
C1	E1	E2
C2	E3	E4

Table 2. Loading configurations

Six service loading tests were conducted and the final ultimate load condition test was performed in load configuration C1. While all service loading configurations were carried out under load-control conditions, the ultimate load condition test was executed through displacement-control in order to best capture the post-peak behavior and to prevent sudden failure. Photographs demonstrating the test set-up are provided in Figure 3.

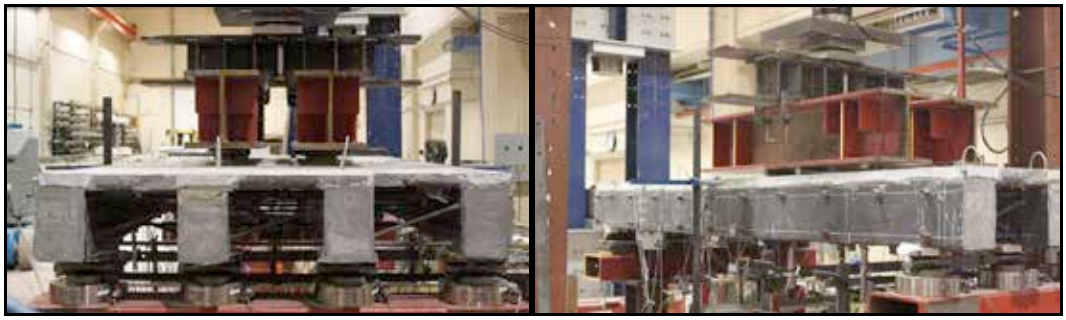

Figure 3. Photographs of ultimate loading condition experimental set-up

Prior to testing of the specimen, an initial average jacking tensile strain equal to 1260 με was applied to all of the PT GFRP rods; after allowing for stress relaxation, the final average

tensile strain in the PT GFRP rods was equal to 926 με. These strain levels were equal to 14% and 10% of the ultimate tensile strain [6] for the GFRP rods at jacking and after stress relaxation, respectively.

4. Experimental Test Results

4.1 Service Loading Configurations

The mid-span vertical deflection and tensile strain in the PT GFRP rods along the transverse cross-section at mid-span were collected during testing of the service loading configurations. The mid-span deflections for each loading configuration during the final service loading cycle (maximum applied load of 50 kN) are provided in Figure 4.

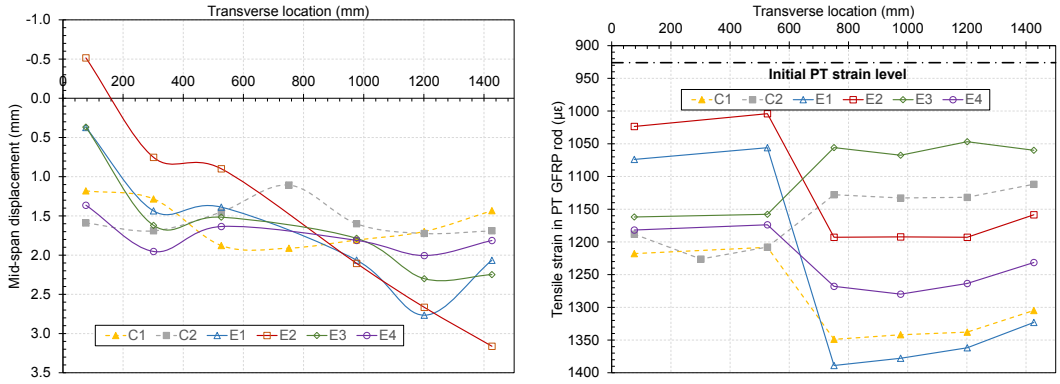

Figure 4. Performance of hybrid bridge deck system at maximum applied service loading: mid-span deflection (left) and tensile strain in PT GFRP rods (right)

Overall, the vertical deflection at mid-span for all loading configurations corresponded to the expected behavior, where greater deflection was observed in areas immediately below the location of the applied load, for both concentric and eccentric configurations. Good load distribution was exhibited in the hybrid bridge deck system, as observed through the smooth transitions of deflection in the specimen. It is worthwhile to note that, in the case of load configuration C2, when the transverse spacing of the wheel loads was doubled from that of loading configuration C1, a reversal in deflection was detected over the middle of specimen; this may result in tensile failure of the UHPC to occur if loaded to ultimate condition in this specific configuration. From initial inspection, it is clear that, in the case of tensile strain in the PT GFRP rod, two distinct zones were present in Figure 4. Significantly reduced tensile strains occurred in the "left" portion of the specimen (between 0 and 600 mm) beyond which a jump in tensile strain was observed for all loading configurations. This phenomenon was attributed to a complication during the construction process, where the cast-in-place UHPC stiffener blocks in select locations seeped into the plastic ducts surrounding the unbonded PT GFRP rod. This caused partial bonding to occur in those zones, resulting in additional fixity constraint to the rod and thus deviations from the expected behavior to occur.

4.2 Ultimate Loading Condition

Progressive failure occurred in the hybrid bridge deck system. Upon reaching the peak load, buckling of the cross-bracing at mid-span occurred, followed by shearing in the web of the GFRP hollow box beams, particularly in the areas of intersection with the transverse GFRP rods where tension shear block failure mechanism was observed. Failure in some of the PT GFRP rods occurred at the interface between the interior rod core and the transverse

threading, causing the portion of the threading embedded within the nuts to slide out; this was the expected failure mode for these GFRP rods, as determined from previous testing [6]. In some locations along the hybrid bridge deck system, the GFRP nuts debonded completely from the PT GFRP rods. With additional applied vertical load, tensile failure occurred in the top surface of the UHPC slab, exhibiting a behavior similar to that of punching shear. The global load-displacement performance of the hybrid bridge deck system is shown in Figure 5, where the relationship between the total applied actuator force and stroke is provided. Representative photographs showing the failure areas are provided in Figure 6.

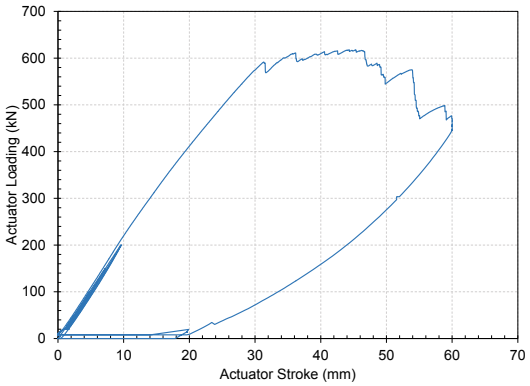

Figure 5. Load-displacement behavior for hybrid bridge deck system up to ultimate

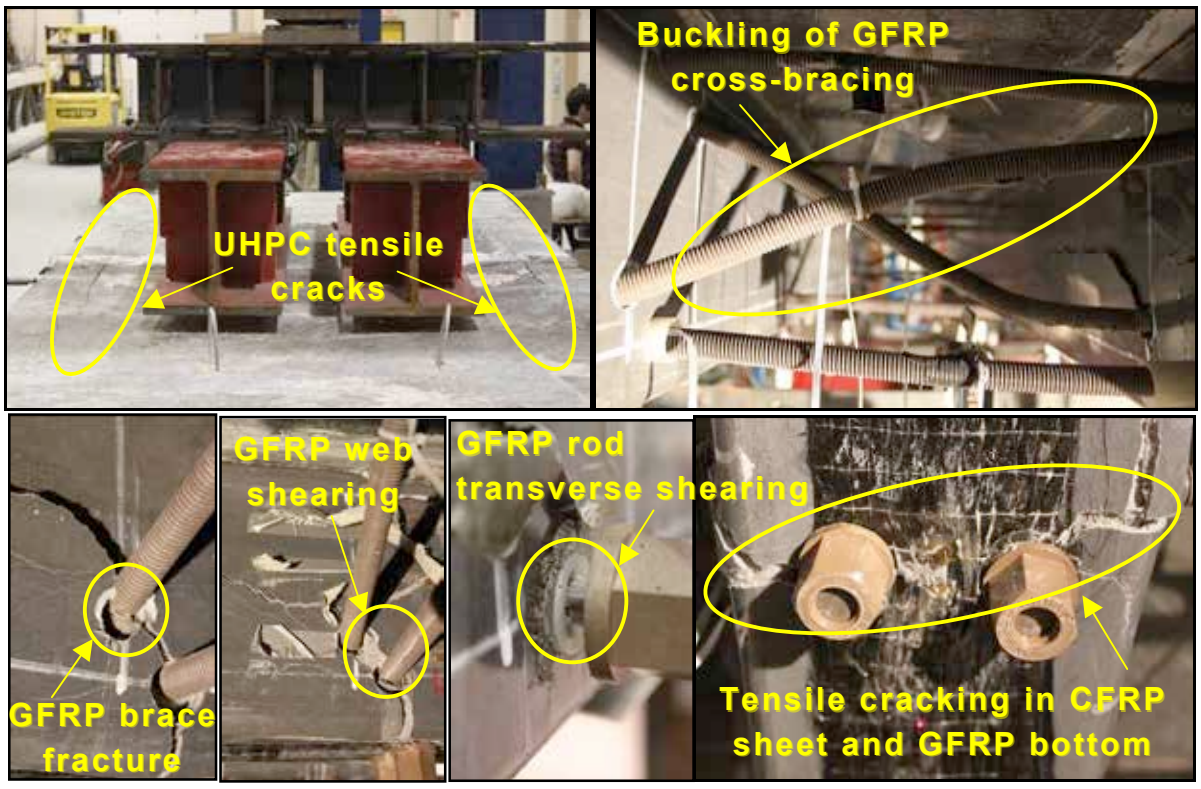

Figure 6. Photographs of the hybrid bridge deck system at failure, with close-ups of failure zones

For closer inspection of local behaviors, the mid-span vertical displacement of the hybrid bridge deck system as well as the tensile strain experienced in the PT GFRP rods located at mid-span during the ultimate condition test are provided in Figure 7 at regular load intervals. Additionally, the performance of the cross-bracings at both the mid-span as well as at the end of the hybrid bridge deck system are presented in Figure 8.

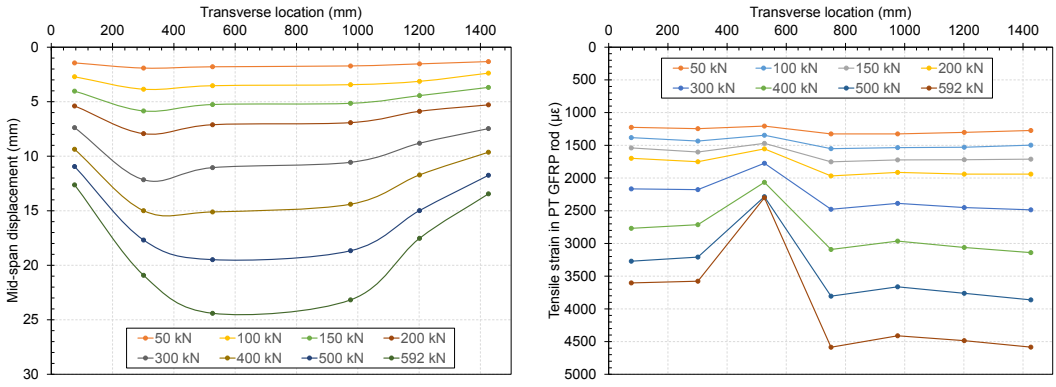

Figure 7. Performance of hybrid bridge deck system at regular load intervals during ultimate load testing: Vertical displacement (left) and PT GFRP rod tensile strain (right) at mid-span

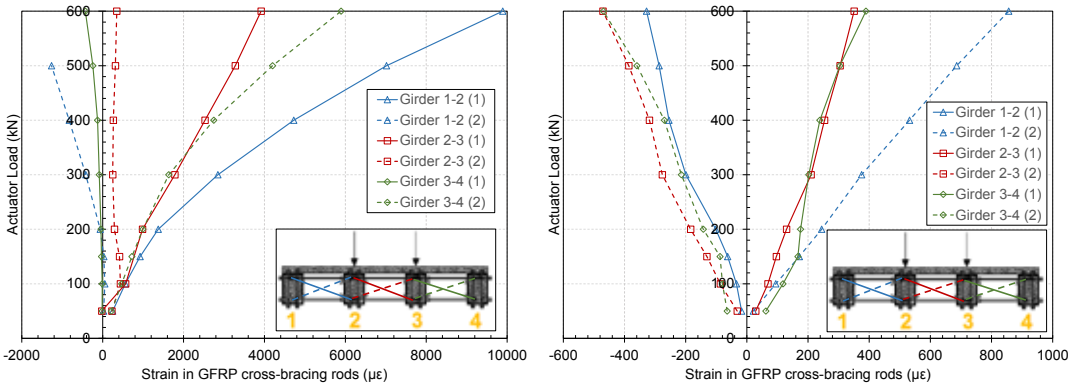

Figure 8. Performance of GFRP cross-bracing rods during ultimate load testing for cross-bracing located at mid-span (left) and at beam end (right)

The displacement and strain values from Figure 7 are consistent with the results obtained in loading configuration C1 under service load. As previously noted, a fixity point was present in the mid-span PT GFRP rod duct at approximately 600 mm from the "left" of the specimen, which caused significantly lower strain values to be experienced at that point. The data presented in Figure 8 confirm that the cross-bracing system performed well to maintain transverse composite action. At the beam end, GFRP cross-bracing rod pairs in each section assumed directly opposing compressive/tensile forces. At the mid-span, due to its proximity to a concentric set of applied loading, large positive moment forces were present in the middle section causing both GFRP cross-bracing rods to perform in tension.

5. Analysis and Discussion of Results

5.1 Overall Performance

Despite the onset of failure in various local areas of the hybrid bridge deck system, the specimen continued to provide load resistance to no less than 70% of its ultimate capacity, while sustaining double the vertical displacement applied at peak load. It is expected that the specimen would have continued to carry load at higher vertical deflection levels if testing progressed until complete collapse of the structure. Thus, the goal of providing pseudo-ductility to a system composed solely of linear-elastic materials was achieved. Comparison of the test results obtained from the service loading configurations confirmed that, with applied service loading no greater than 10% of the ultimate capacity, the hybrid bridge deck system behaved linear-elastically, locally and globally, and did not retain residual strains. In general,

the performance of specimen was as expected for all of the different loading configurations tested, and the additional fixity exerted on the mid-span PT GFRP rod at 600 mm from the "left" side of the specimen did not affect the global performance of the system.

Judging from the data obtained from the PT GFRP rods, it was found that at ultimate and service loading conditions under load configuration C1, the rods utilized approximately 44% and 15% of its tensile capacity [6]. Damage in the PT GFRP rods was observed to occur only in nut-thread connections. Similarly, the GFRP straps would have utilized a far lower portion of their ultimate capacity, since post-tensioning was not applied to the straps and because their spacing density was higher than those of the PT rods were. Therefore, further design optimization should be performed to examine the feasibility of increasing the overall tensile strain induced in the PT GFRP rods and GFRP straps in order to maximize the performance of each structural component while minimizing costs. In the case of the GFRP cross-bracing rods, buckling occurred once compressive strains exceeded approximately 1000 με, as seen in Figure 8. Therefore, more rigorous examination of the induced compression forces in the cross-bracing rods should be performed using extrapolation of data obtained from the five other service loading configurations in order to determine if buckling is a serious concern at ultimate capacity. If so, a redesign of the girder spacing in the transverse direction or the rod size may be required to ensure adequate performance of the hybrid bridge deck system.

5.2 Load Distribution Factors

Another aspect of multi-girder bridge design is load allocation between the main girders. The shear force distribution factor between the four parallel girders is presented in Figure 9.

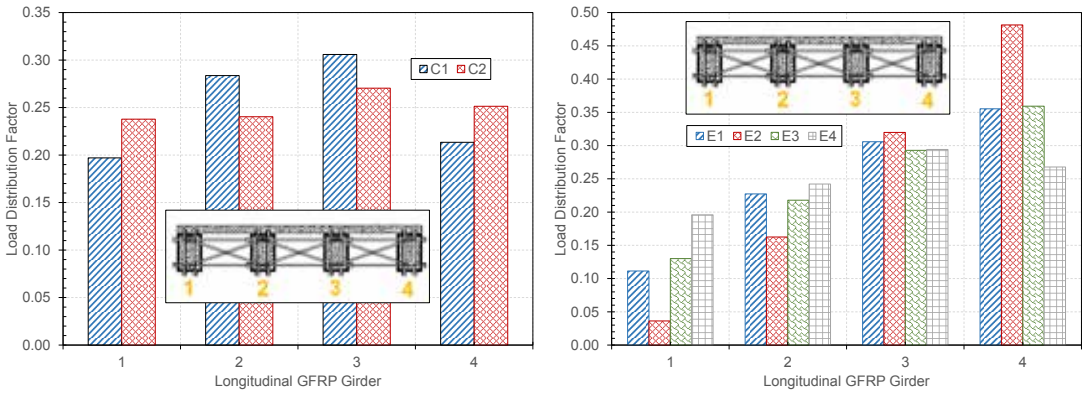

Figure 9. Shear force distribution factor for concentric configurations (left) and eccentric configurations (right)

Smooth load distribution amongst the longitudinal girder was experienced for all of the loading configurations. For concentric loading, near even load distribution was observed, particularly in the case of load configuration C2 (25% of load carried per girder) where a wider placement of wheel loads was used. In the case of the eccentric loading configurations, higher load was taken up by the girders closest to the applied load, where a maximum load distribution factor of almost 50% was taken up by the outer girder (Girder 4) in load configuration E2. Overturning did not occur for all eccentric loading configurations.

6. Conclusions

Experimental testing of the 3m long hybrid bridge deck specimen showed good global performance of the designed system. Specific conclusions include:

1. Successful incorporation of pseudo-ductility into a system composed entirely of linear-elastic materials, with a progressive failure mechanism in effect at ultimate, resulting in a sustained load resistance in excess of 70% of the peak load reached;
2. Strong transverse composite action achieved through the use of horizontal PT GFRP rods, horizontal non-prestressed GFRP straps and diagonal GFRP cross-bracing rods;
3. Consistent distribution of shear load across the four parallel girders under concentric loading (25% load carried per girder), with an outer girder expected to carry 50% of the load applied when subject to the most eccentric loading configuration;
4. Optimization of PT GFRP rod and GFRP strap spacing can be performed to increase structural efficiency since a maximum of 44% of the ultimate tensile strain in the GFRP rods was utilized in the present design; and,
5. Buckling in the cross-bracing rods may initiate the progressive failure mechanism in other loading configurations when subjected to ultimate loading.

For future study, the authors recommend that the effect of dynamic and impact loading on the hybrid bridge deck system be explored. Additionally, determining its performance in a continuous span application, thus resulting in negative moment over interior supports, would be greatly beneficial to the state-of-the-art of hybrid bridge design.

7. Acknowledgements

The authors would like to thank Lafarge Canada for their generous donation of materials used. We would also like to acknowledge the University of Calgary and the Natural Sciences and Engineering Research Council of Canada (NSERC) for their financial support. Lastly, we would like to thank the technical staff for their invaluable help during experimental testing.

References

[1] ACI. *Load tests of concrete structures: methods, magnitude, protocols, and acceptance criteria (ACI 437.1 R-07)*. Farmington Hills, 2007.
[2] A. Elmahdy. *Experimental and analytical study of new hybrid beam constructed from high performance materials*. Doctor of Philosophy Dissertation. University of Calgary, 2010.
[3] CSA. *Canadian Highway Bridge Design Code (CSA S6-06)*. Mississauga, 2006.
[4] D. Chen and R. El-Hacha. Behaviour of hybrid FRP-UHPC beams in flexure under fatigue loading. *Composite Structures*, 94(1):253-266, 2011.
[5] D. Chen and R. El-Hacha. Bond strength between cast-in-place Ultra-High-Performance-Concrete and Glass Fibre Reinforced Polymer plates using epoxy bonded coarse silica sand. *Journal of ASTM International*, 9(3):1-19, 2012.
[6] D. Chen and R. El-Hacha. Performance of post-tensioned GFRP threaded rods for bond applications. In *the Seventh International Conference on FRP Composites in Civil Engineering*, 6 pages, 2014. (Accepted)
[7] J. Lee, Y. Kim, J. Jung and J. Kosmatka. Experimental characterization of a pultruded GFRP bridge deck for light-weight vehicles. *Composite Structures*, 80(1):141-151, 2007.
[8] N. Deskovic, T.C. Triantafillou and U. Meier. Innovative design of FRP combined with concrete: Short-term behavior. *ASCE Journal of Engineering*, 121(7):1069-1078, 1995.
[9] R. El-Hacha and D. Chen. Behaviour of hybrid FRP-UHPC beams subjected to static flexural loading. *Composites Part B: Engineering*, 43(2):582-593, 2012.
[10] W. Alnahhal and A. Aref. Structural performance of hybrid fiber reinforced polymer-concrete bridge superstructure systems. *Composite Structures*, 84(4):319-336, 2008.